LAWRENCE
LIVERMORE
NATIONAL
LABORATORY

UCRL-CONF-201173

Towards An Ideal Slow Cookoff Model For PBXN-109

J. J. Yoh, M. A. McClelland, J. L. Maienschein, A. L. Nichols, J. F. Wardell

November 25, 2003

JANNAF 2003
Colorado Springs, CO, United States
December 1, 2003 through December 5, 2003

TOWARDS AN IDEAL SLOW COOKOFF MODEL FOR PBXN-109[1]

J. J. Yoh, M. A. McClelland, J. L. Maienschein, A. L. Nichols, and J. F. Wardell
Energetic Materials Center
Lawrence Livermore National Laboratory
Livermore, CA

ABSTRACT

We present an overview of computational techniques for simulating the thermal cookoff of high explosives using a multi-physics hydrodynamics code, ALE3D. Recent improvements to the code have aided our computational capability in modeling the response of energetic materials systems exposed to extreme thermal environments, such as fires. We consider an idealized model process for a confined explosive involving the transition from slow heating to rapid deflagration in which the time scale changes from days to hundreds of microseconds. The heating stage involves thermal expansion and decomposition according to an Arrhenius kinetics model while a pressure-dependent burn model is employed during the explosive phase. We describe and demonstrate the numerical strategies employed to make the transition from slow to fast dynamics. In addition, we investigate the sensitivity of wall expansion rates to numerical strategies and parameters. Results from a one-dimensional model show increased violence when the gap between the explosive and steel vessel is removed.

INTRODUCTION

In the DoD/DOE communities, there is an interest to employ computer simulations to reduce the number of experiments for weapons design and safety evaluation. One area of great success in modelings and simulation is the characterization of munitions exposed to extreme conditions, such as shocks and detonations. Hydrocodes, which are designed to simulate the high-frequency response involving initiation and propagation of shocks and detonations, have been used extensively in the energetic materials community.

The low-frequency response of energetic materials, on the other hand, has yet to be well modeled. This process, characterized by the slow response of the system under thermo-mechanical loading, is essentially a quasi-static process that goes from an initial to a final state through a series of equilibrium states. In practice, a quasi-static process must be carried out on a time scale which is much larger than the relaxation time of the system. Modeling of the entire process of slow to fast dynamics requires the coupling of low-frequency response of an energetic system to the equilibrium time scale of momentum transport. Typical time steps involved in this process vary by several orders of magnitude, and in particular,

$$\Delta t\|_{\text{motion}} << \Delta t\|_{\text{system}}. \tag{1}$$

The multi-time scale behavior encountered of interest is the cookoff of high-explosive (HE) systems [1, 2, 3, 4, 5]. For example, the Navy is interested in the behavior of munitions in shipboard fires to help with the design of storage systems and the development of fire fighting procedures. In these fires, time scales for behavior can range from days to microseconds. During the relatively slow heating phase, the response of an energetic materials system is paced by thermal diffusion and chemical decomposition while the mechanical response is essentially a quasi-static process. As the decomposition reactions accelerate, heat is generated faster than it can be removed. Product gases

[1] Approved for public release; distribution is unlimited. The work was performed under the auspices of the U.S. Department of Energy by the University of California, Lawrence Livermore National Laboratory under Contract No. W-7405-Eng-48.

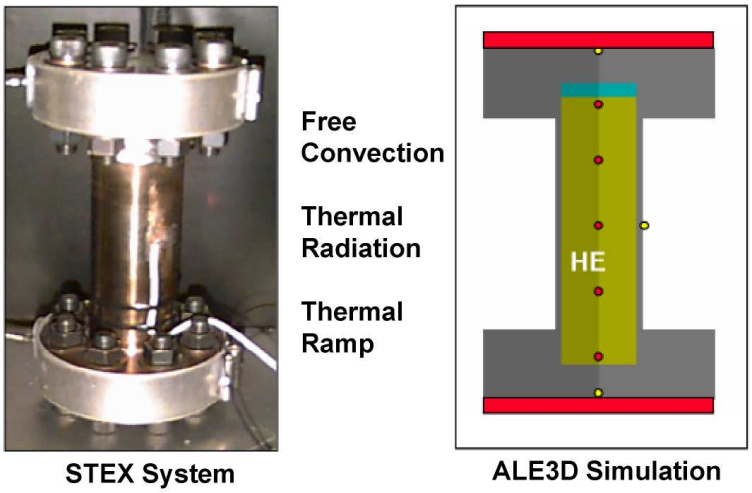

Figure 1. Photograph of the STEX system (LEFT) for the ALE3D model (RIGHT) validation experiment.

are formed and the resulting pressure rises accelerate the energetic and containment materials. The resulting violence can range from a pressure rupture to a detonation.

The accurate modeling and simulation of cookoff requires an understanding of the mechanical, thermal, and chemical behavior during slow heating and the subsequent explosion [1, 3, 6]. The explosion time and temperature have been successfully predicted using relatively simple thermal analysis codes [7]. However, the prediction of reaction violence requires detailed mechanical models throughout the cookoff event. In particular, dynamic gaps and the generation of thermal damage (porosity and cracks) during slow heating are likely to be important factors. These processes are typically orders of magnitude slower than those associated with the burn phase. Thus, to model a slow cookoff event will require computational tools and models that can handle a wide variety of physical processes and time scales.

In this paper, we describe how the cookoff of high explosives is simulated with the arbitrarily Lagrangian-Eulerian code [8, 9], ALE3D. In particular, we discuss the numerical methodology to transition from slow to fast time scales. We apply our modeling capability to a Scaled Thermal Explosion Experiment (STEX) [4] and compare calculated and measured curves for the wall strain during both the heating and explosive phases of the test.

DESCRIPTION OF THE STEX EXPERIMENT

The STEX is designed to quantify the violence of thermal explosions under carefully controlled conditions, and to provide a database which we can use to validate predictive codes and models [4]. A cylindrical test, shown in Fig. 1, is devised where the ignition starts in the axially central region of the cylinder. The confinement vessel consists of a steel wall and end caps with known mechanical properties that are insensitive to temperature. A constant length to diameter ratio of 4:1 is used. For a charge of 5.08 cm diameter, 20.3 cm length, the respective wall thickness was 0.4 cm. A 5 % gap is provided in the upper part of the vessel to allow the HE to expand freely before ignition. Three radiant heaters are used to control the wall temperature. Each end cap is heated with a separately controlled heating device.

Table 1. Chemical kinetics parameters for model PBXN-109

Reaction step	$\ln Z_k$	E_k (kcal/g-mole-^{O}K)	q_k (cal/g)
$A \rightarrow B$	$30.02\,\mathrm{s}^{-1}$	46.5	64 (endothermic)
$B \rightarrow C + Al$	$25.22\,\mathrm{s}^{-1}$	43.6	-192 (exothermic)
$C \rightarrow D$	$19.02\ \mathrm{cm}^3/\mathrm{s\text{-}g}$	33.7	-1013 (exothermic)

MODEL FOR PBXN-109

ALE3D chemical, mechanical, and thermal models are developed to model the cookoff of PBXN-109. The decomposition of PBXN-109 is modeled by three-step, four-species chemical kinetics based on pure RDX model reported in [7]. The mechanical models for the solid chemical constituents along with the steel components are taken to have Steinberg-Guinan [10] strength models in which a polynomial expression is used for the equations of state. The gaseous products are treated as no-strength materials with gamma-law equations of state. The time-dependent thermal transport model includes the effects of conduction, reaction, advection, and compression. The thermal conductivity for the HE solid species is taken to be constant, whereas the effects of temperature are included for the gaseous species. The air in the gaps between the HE and the steel case is modeled with a Gamma-Law model. The parameters in these models were determined from measurements as reported in [1, 2].

The three-step, four-species reaction mechanism for PBXN-109 is

$$A \rightarrow B \qquad r_1 = Z_1 \exp(-E_1/RT)\,\rho_{\mathrm{A}} \tag{2}$$

$$B \rightarrow C + Al \qquad r_2 = Z_2 \exp(-E_2/RT)\,\rho_{\mathrm{B}} \tag{3}$$

$$C \rightarrow D \qquad r_3 = Z_3 \exp(-E_3/RT)\,\rho_{\mathrm{C}}^2 \tag{4}$$

where A and B are solid species, and C and D are product gases. In the second reaction step, aluminum, Al, is separated from the reactant B without reacting. The rate parameters above are adjusted to fit the One-Dimensional-Time-to-Explosion (ODTX) measurements [11], and they are given in Table 1.

The comparison of measured and calculated ODTX results for PBXN-109 is shown in Fig. 2. Original Fit corresponds to a set of kinetics parameters reported earlier [1], and Zero Endotherm corresponds to the special case of zero heat of reaction for first reaction, $q_1 = 0$. The solid curve represents explosion times calculated with the present chemical kinetics for the case of reaction and thermal transport without material motion. Though all three curves are similar, the present curve is shifted downward from the Original Fit, indicating that the ignition time will be shorter.

After the chemical reactions have progressed significantly into the faster regime of cookoff where changes are occurring on the time scale of the sound speed, a switch is made to a burn front model in which reactants are converted to products in a single reaction step. The burn front velocity, V is assumed to be a function of pressure only, and it takes the form

$$V = V_0 \left(\frac{P}{P_0} \right)^n . \tag{5}$$

Here the subscript 0 indicates a reference quantity. The parameters used in the current simulation are,

$$V_0 = 1.0 \times 10^{-1}\ \mathrm{m/s} \quad \text{(for thermally damaged PBXN-109)}$$

$$V_0 = 5.0 \times 10^{-3}\ \mathrm{m/s} \quad \text{(for pristine PBXN-109)}$$

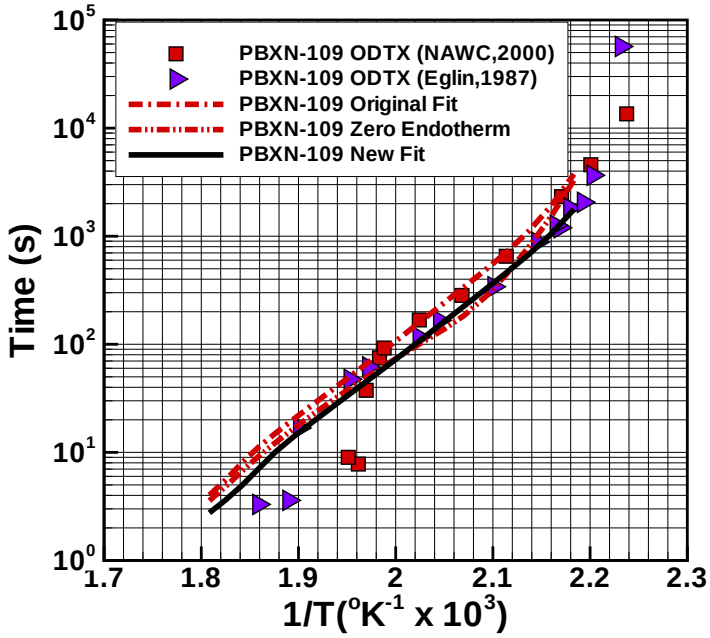

Figure 2. Comparison of ODTX measured and calculated results for PBXN-109

$$P_0 = 0.1 \text{ MPa}, \qquad n = 1.46$$

Here the coefficient V_0 has two possible values. For damaged material, the coefficient is increased by a factor of 20 from the pristine material value. Burn rate data for pristine and thermally-damaged HE are bounded by the two lines in Fig. 3. The data in the figure show an increase in deflagration rates of up to 20 fold for thermally damaged samples. All samples showed this very fast deflagration for about the first third of the sample, with the remainder of the sample burning at rates about the same as or slightly slower than the pristine material. In the current simulations, the burn rate represented by the lower curve is used to model the deflagration of PBXN-109 sample during the fast expansion.

NUMERICAL STRATEGY FOR COOKOFF SIMULATIONS

Fig. 4 shows one and two-dimensional modeling domains for a STEX test involving PBXN-109 (64 % RDX, 20 % Al, 16 % DOA/HTPB). A wedge slice is taken from the center line of the STEX system shown in the right image. This one-dimensional wedge represents an axisymmetric section of the STEX system in which variations occur only in the radial direction. The boundaries at planes of constant θ are rigid slip surfaces. In the experiment [4], the HE, nominally 5.08 cm diameter is encased in a 0.4 cm thick steel cylinder. The 5 % ullage by volume is located at the outside radius of the HE in the 1D model. The gaps are treated in two different ways in the 2D models. In Model 2Da, a 4 % gap by volume is included at the top end of the cylindrical charge, and a 1 % gap is used at the outside radius of the HE. In Model 2Db, a 5 % gap is included at the top of the cylinder, and there is no gap on the side.

The cookoff simulation starts with a gradual increase of the set-point temperature at the steel surface to $130\,^{o}$C, followed by a hold for 5 hours, and then an increase at a rate of $1\,^{o}\text{C}/\text{h}$ until cookoff. As the PBXN-109 is heated, it thermally expands to fill in the gap. At a temperature above $130\,^{o}$C, exothermic decomposition begins and eventually ignition occurs near the midplane of the system. On a

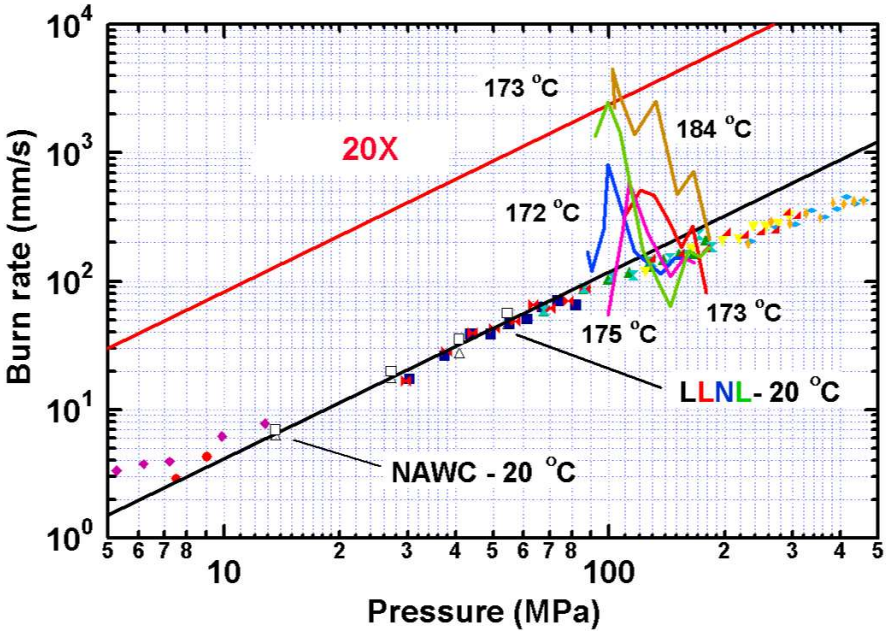

Figure 3. Burn rate data for PBXN-109 for pristine and heated samples

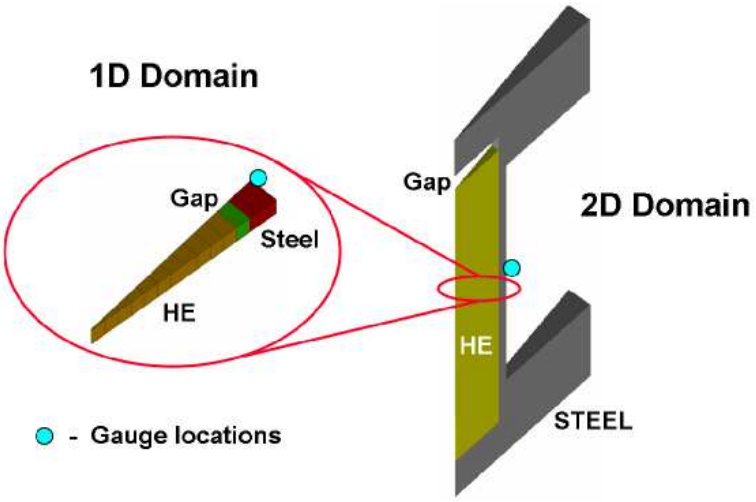

Figure 4. Schematics of 1D and 2D domains. 1D mesh is generated from a slice along the center radial line of 2D mesh on the right column. In both, 5 % gap (by volume) is added between the HE and the steel casing.

time scale of microseconds, the propagation of flame through the PBXN-109 causes the temperature and pressure to rise, and ultimately causes a break in confinement.

In the simulations, four different mesh resolutions (1X, 2X, 4X, 8X) are considered. In the base case (1X), there are 12 elements across the HE in the radial direction, and in the fine mesh case there are 96 elements in this direction. The air/HE interface is not tracked explicitly, and zones with both air and HE have properties determined by the mixing rule discussed next.

STRAIN ALLOCATION FOR MIXED ELEMENTS

In real systems, there are gaps present between the HE sample and its case. Whether the presence of gaps is by design or not, its effect in the cookoff violence is believed to be significant. It is important to treat gaps or voids in all calculations related to cookoff. The ALE3D code has two ways of modeling gaps. The first way uses a standard sliding contact algorithm that makes use of the concept of slave / master surfaces. The gap surfaces are 'tracked' in this case. The second way of treating gaps is the mixed element approach that we use in this work. Instead of tracking the sharp interface, the element values are allowed to 'diffuse' across the interface. Although typically higher mesh resolution is needed, the mixed-element approach can provide accurate results when properly applied.

We consider a mixed element consisting of material (1) and material (2) (see Fig. 5). The material (1) may represent HE and material (2) may be air or void. The addition of strains in the direction normal to this interface can be described by

$$\dot{\varepsilon}_1' L_1 + \dot{\varepsilon}_2' L_2 = \dot{\varepsilon}' L$$

where $\dot{\varepsilon}'$ denotes total strain rate, and L represents the length of the mixed element between two materials. Assuming equal areas, we can rewrite the strain rates using the volume fraction, f, namely,

$$\dot{\varepsilon}_1' f_1 + \dot{\varepsilon}_2' f_2 = \dot{\varepsilon}'.$$

Using the stress-strain relationship and assuming equal stress rates across any material interface, we write the above expression as

$$\frac{f_1}{\mu_1} + \frac{f_2}{\mu_2} = \frac{1}{\mu_{\text{eff}}} \tag{6}$$

where μ_{eff} is the effective shear modulus for the mixture. The effective stress rate is then given by

$$\dot{\sigma}_{\text{eff}}' = \mu_{\text{eff}} \dot{\varepsilon}' = \dot{\sigma}_1' = \dot{\sigma}_2'.$$

Then the component strain rates are given by

$$\dot{\varepsilon}_1' = \frac{\mu_{\text{eff}} \dot{\varepsilon}'}{\mu_1} \text{ and } \dot{\varepsilon}_2' = \frac{\mu_{\text{eff}} \dot{\varepsilon}'}{\mu_2}. \tag{7}$$

Because the air gap is modeled as a very soft material with finite strength, that is $\mu_{\text{HE}} >> \mu_{\text{air}}$, the component strain rates become

$$\dot{\varepsilon}_{\text{air}}' \approx \frac{\dot{\varepsilon}'}{f_{\text{air}}} \text{ and } \dot{\varepsilon}_{\text{HE}}' \approx 0. \tag{8}$$

FINDING A SUITABLE SCALING FACTOR

The equations of mass, momentum, energy, and chemistry are solved on the long time scale of the heating phase and on the short time scale of the thermal runaway phase in a single simulation. The momentum equation is integrated explicitly during both the slow and fast phases. In order to provide computationally feasible step sizes , the method of variable mass scaling [12] is applied during the slow heating phase. The density is increased in the momentum equation to reduce the sound speed and allow larger step sizes consistent with the Courant condition. However, if the time step size and material density are too large, spurious fluctuations, characteristic of a simple harmonic oscillator, appear. Thus, a tradeoff is required between numerical efficiency and accuracy. In practice, the time step size is fixed during the slow heating phase with the density calculated from the Courant condition.

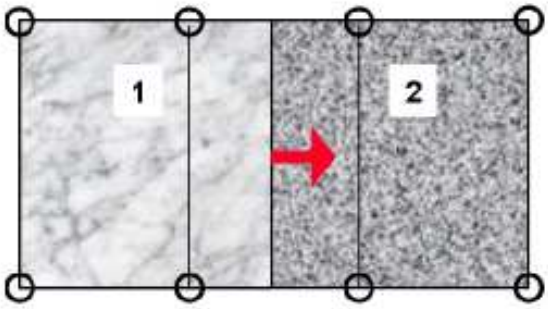

Figure 5. Strain allocation model distributes nodal strain rates based on the material elastic moduli.

Table 2. Material properties used in the cookoff simulation. Shown are the density (ρ), coef. of thermal expansion (CTE), shear modulus (μ), and yield strength (Y_0).

	ρ (g/cm^3)	CTE ($^oC^{-1}$)	μ (GPa)	Y_0 (GPa)
PBXN-109	1.67	1.21e-4	4.628e-3	0.06
Steel 4340	7.83	1.20e-5	77.0	1.03

During the transition phase in which the decomposition reactions are accelerating, the time step size is reduced to meet error specifications for the calculation of thermal and composition fields. At the same time, the artificial density is reduced following the Courant condition until the physical value is obtained. When the HE reaches a user-specified temperature, the Arrhenius kinetics expression are replaced by a burn model. A level-set method is used in the modeling of the advancing burn front.

We use the Backward Euler method for the integration of the thermal equations and reaction kinetics during the heating, and transition phases. During the slow heating phase, the time step size is the value selected for the integration of the hydrodynamic equations. A switch is made to an explicit method when the time step size is a user-specified multiple of the Courant time step size calculated with no mass scaling.

RESULTS AND DISCUSSION

ONE-DIMENSIONAL ANALYSIS

Calculated results for the wall hoop strain are shown in Fig. 6 for the one-dimensional STEX test. For comparison, the theoretical thermal expansion of an empty steel vessel is shown in the same plot. In order to study the effect of a gap, we calculate strains for systems with and without gaps. In the figure, there is a clear evidence of increase in strain when the system has no gap during the slow thermal phase. The resulting strain when a gap is included (shown in solid red) is smaller by a factor of two or more during the same time period. The strain curve coincides with the analytical expansion of pure steel (shown in blue) up to about 40 hours. As the temperature increases, the HE thermally expands inside the steel vessel at a rate approximately 10X greater than the steel vessel itself (see Table 2). An estimated time of contact at which the unreacted PBXN-109 fills the 5 % gap and starts pushing on the steel wall is approximately 53 hours. Since the solid HE undergoes the chemical decomposition described earlier and the decomposition gases pressurize the vessel, the overall strain values are greater than the analytical expansion of the steel vessel alone.

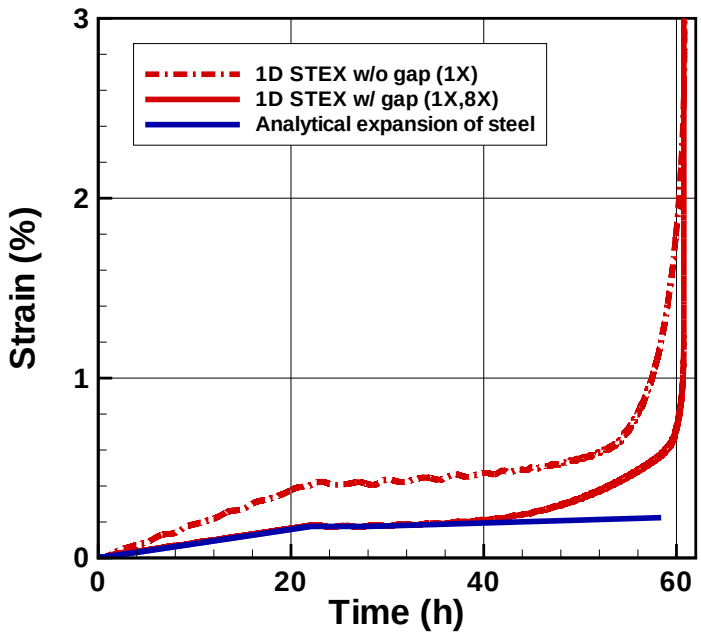

Figure 6. Simulated mechanical response of confined explosive in a 1D STEX experiment. The two strain calculations show excellent agreement until about 40 hours as chemical decomposition of PBXN-109 becomes pronounced in the confined system.

In Fig. 7, we plot the pressure rise due to the exclusion of a gap in the one-dimensional STEX system. During the first 40 hours, the system with gap experiences no significant pressure increase. This observation supports the claim that the presence of gaps in the STEX system can prevent unwanted over pressurization of the vessel before the ignition takes place. After 40 hours, PBXN-109 continues to undergo chemical decomposition, producing more product gases that further pressurizes the vessel. The increased production of the first gaseous species, X_c, is tied in with the rapid pressure rise in the system as seen from Fig. 8. As unreacted HE species (X_a, X_b) are consumed to generate more hot product gases (X_c, X_d), the pressure as calculated by the Gamma-Law model, starts to increase significantly. At about 62 hours, well into the cookoff phase, both the elevated temperature ($> 2000\,^{o}$K) and the presence of final product gas (X_d) trigger the switching of chemical kinetics to a deflagration burn-front mechanism that rapidly expands the steel vessel during the ignition-burn phase.

Fig. 9 shows the second phase, the fast burning phase of the slow cookoff process (see Fig. 6). The effect of the presence of gap as seen in the slow phase case is more pronounced, in that, two fast strain rates or the slopes of each curves are distinct for both with and without gaps. If one associates strain rates with flying particle or fragment velocities, the system without gap is clearly marked by a violent reaction while the system with gap experiences a relatively less violent or benign response.

TWO-DIMENSIONAL ANALYSIS

The two dimensional simulations add the influence of variations in the z direction. This system is assumed to be axisymmetric, and a cylindrical wedge was selected for the calculation domain. In Fig. 10, the calculated thermal response of the STEX system is shown together with measured data. The system is heated from room temperature to 50 ^{o}C at a rate of 3.35 ^{o}C/h, followed by a 1.67 hour soak. Then at a ramp rate of 3.77 ^{o}C/h, the system temperature rises to 130 ^{o}C, followed by a 5 hour soak.

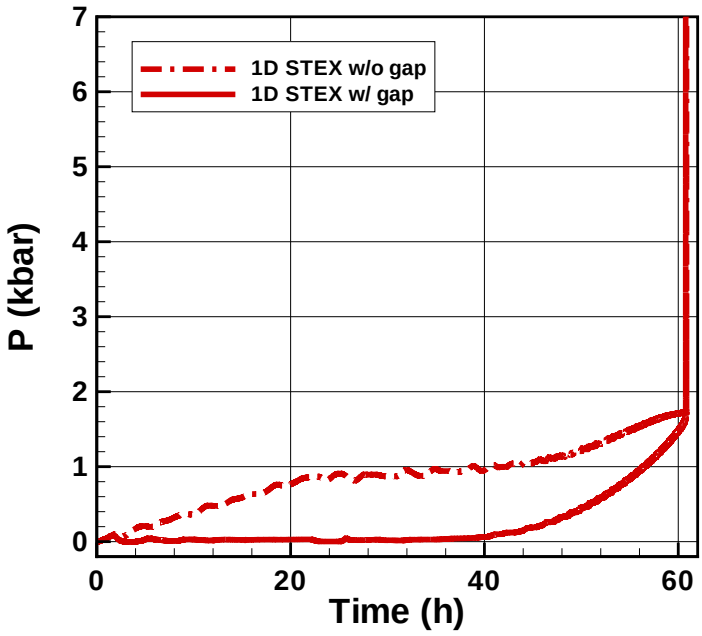

Figure 7. In both cases, the pressure starts to rise again at around 40 hours.

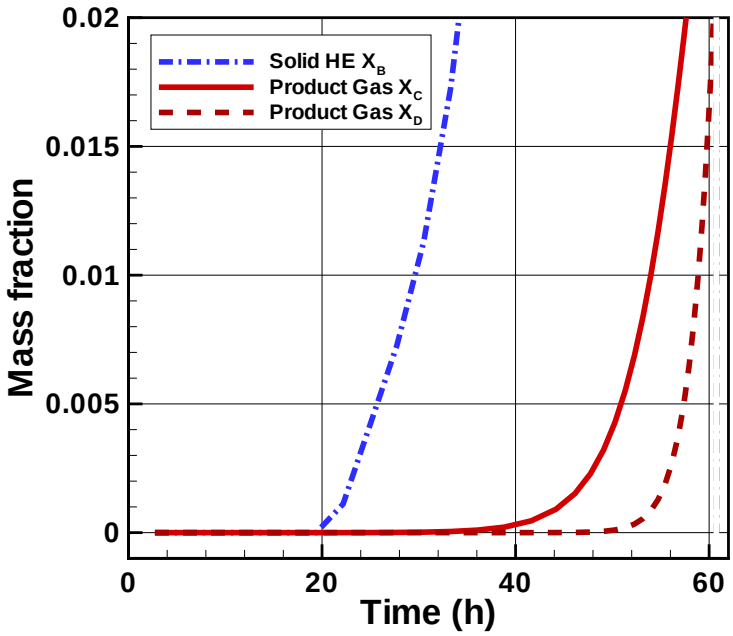

Figure 8. Formation of gaseous product X_C at about 40 hours marks the onset of pressure increase in the 1D STEX system with gap.

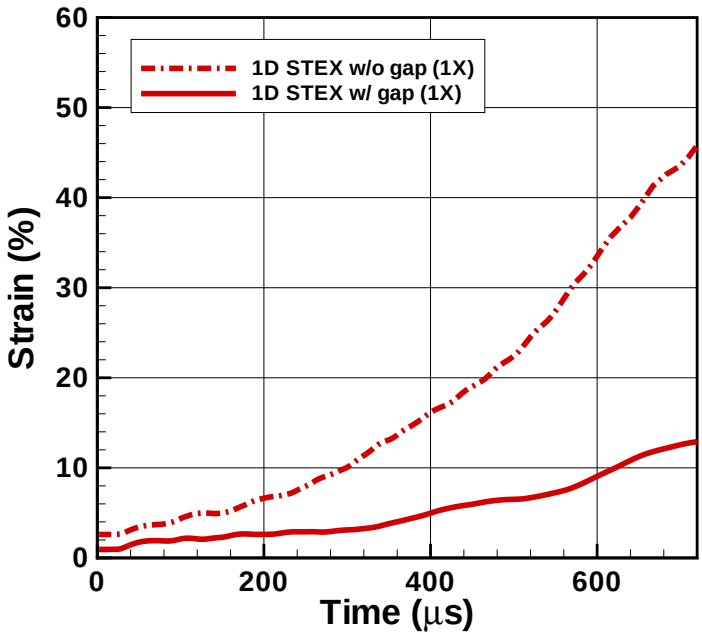

Figure 9. Simulated mechanical response of confined explosive in a 1D STEX experiment. The system with gap shows remarkably slower strain rates than the system without gap.

Then the final heating phase at a rate of 1 ^{o}C/h is maintained until explosion. The measured and calculated thermal responses generally agree except that the calculated ignition temperature is higher than the measurement by 5 degrees.

In Fig. 11, calculated wall hoop strains for the STEX system are presented together with the measurements. As was done for the one-dimensional case, the theoretical expansion of the empty steel vessel is plotted as well. Shown are the hoop strains for Model 2Da on meshes of four different resolutions. These results are generally higher than the measurements, and show spurious oscillations from the method of mass scaling used in the integration of the momentum equations described before. The results for the four meshes appear to be approaching a converged solution, but full convergence has not yet been achieved at 8X mesh resolution. The results for Model 2Da, should match the empty vessel results until the 1 % gap at the side of the HE cylinder closes at $t = 9.4$ hours and a strain of 0.056 %. It is seen that the Model 2Da curves are higher than the empty vessel curve during this period, indicating that numerical errors of the scale 0.1 % remain.

A rapid expansion of the vessel wall follows the slowing heating and ignition phases. In Fig. 12, wall strain results for Model 2Db (no side gap) are compared with the measured hoop strain results for the STEX test. Shown are the calculated strain using the 4X mesh and the measurement. The model results compare favorably with the measured results until $t = 275\,\mu$s. At this time, the measured strain rate changes dramatically. It is likely that the gauge failed at this point.

Although the model provides a good representation of the measurements, mesh refinement results need to be completed to establish the numerical accuracy of the calculations. Also noted is the challenge to minimize the inherent oscillatory artifacts associated with mass scaling. Oscillation free strain results is possible if an implicit approach is used during the quasi-static process. To generate the smooth looking strain results of Fig. 12, the time step size before the burn was reduced by a factor of

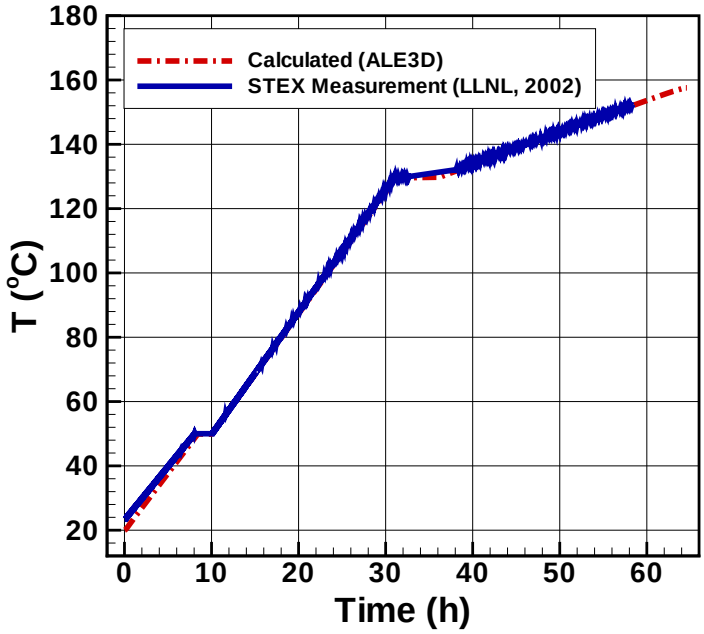

Figure 10. Calculated thermal response of confined HE in a 2D STEX experiment. The predicted ignition temperature is 5 degrees higher than the STEX result.

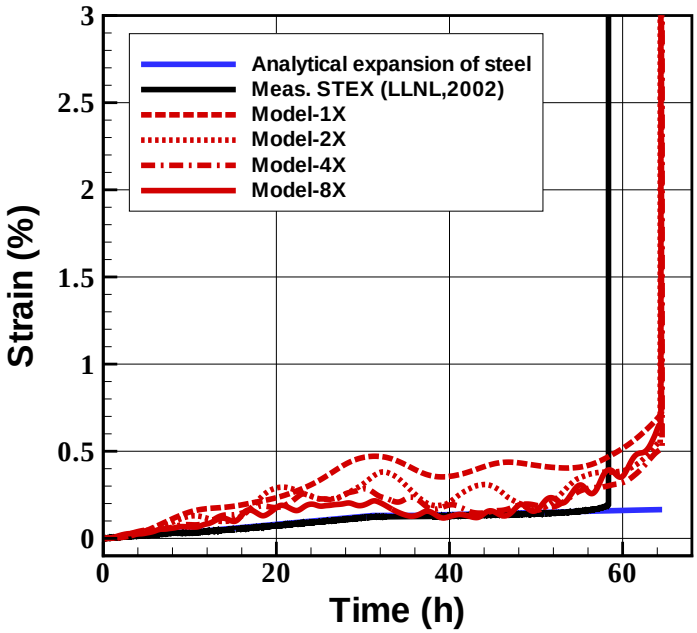

Figure 11. Calculated mechanical response of confined HE in a 2D STEX experiment. The slow heating phase and the initial fast ignition phase. Four levels of mesh refinement are shown with an ideal steel expansion and the measurement.

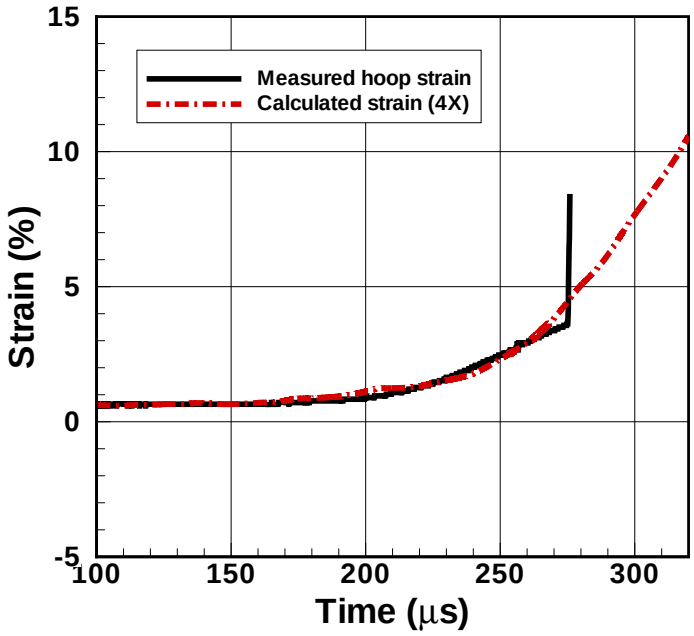

Figure 12. Comparison of measured and calculated hoop strains during a thermal runaway. The experimental strain data is available until about 275 μs where the gauge breaks.

10^3. To overcome this barrier, the implicit hydro approach is being developed for future calculations. Finally, the gap at the side of the HE needs to be added to provide a more complete model of the actual STEX system.

CONCLUSIONS

Progress has been made towards the ideal ALE3D model for cookoff tests. Numerical procedures have been developed to model the thermal, mechanical, and chemical behavior during the slow heating, transition, and explosive phases in a single simulation. In this paper attention is focused on the accuracy of mechanical results for the simulation of a STEX test with PBXN-109. For the heating phase, an explicit hydro scheme with mass scaling provides numerically accurate results for wall strains in one-dimension and approximate results in two dimensions. The one-dimensional results show increased strain rates for the case of no gap. For the rapid expansion, the model provides a good representation of measured wall strains. However, a better treatment of gaps is needed during the heating phase to confirm the numerical accuracy of these model results. An implicit hydro scheme with slide surfaces is being developed to provide improved accuracy for cookoff systems with gaps.

ACKNOWLEDGMENTS

Support for this work was provided by the DoD/DOE Joint Technology Development Program. The work was performed under the auspices of the U.S. Department of Energy by the University of California, Lawrence Livermore National Laboratory under Contract No. W-7405-Eng-48. Discussions with Rich Becker on strain allocation model and with Brad Wallin on slide surfaces are warmly acknowledged.

REFERENCES

1. McClelland, M. A., Maienschein, J. L., Nichols, A. L., Wardell, J. F., Atwood, A. I., and Curran, P. O., “ALE3D Model Predictions and Materials Characterization for the Cookoff Response of PBXN-109,” in *Proceedings of JANNAF 38th Combustion and 20th Propulsion Systems Hazards Subcommittee Meetings*, Destin, FL, 2002.
2. McClelland, M. A., Tran, T. D., Cunningham, B. J., Weese, R. K., and Maienschein, J. L., “Cookoff Response of PBXN-109: Material Characterization and ALE3D Thermal Predictions,” in *Proceedings of JANNAF 50th Propulsion Meeting*, Salt Lake City, UT, 2001.
3. McClelland, M. A., Maienschein, J. L., Nichols, A. L., and Yoh, J. J., “Ignition and Initiation Phenomena: Cookoff Violence Prediction”, UCRL-ID-103482-02, 2002.
4. Wardell, J. F., and Maienschein, J. L., “The Scaled Thermal Explosion Experiment,” in *Proceedings of 12th International Detonation Symposium*, San Diego, CA, Offi ce of Naval Research, 2002.
5. Nichols, A. L., Couch, R., McCallen, R. C., Otero, I., and Sharp, R., “Modeling Thermally Driven Energetic Response of High Explosives,” in *Proceedings of 11th International Detonation Symposium*, Snowmass, Colorado, 1998.
6. Williams, F. A., *Combustion Theory*, Addison-Wesley, Redwood City, CA, 1985.
7. McGuire, R. R., and Tarver, C. M., “Chemical Decomposition Models for the Thermal Explosion of Confi ned HMX, TATB, RDX, and TNT Explosives,” in *Proceedings of 7th International Detonation Symposium*, Annapolis, MD, Naval Surface Weapons Center, 1981, pp. 56–64.
8. Belytschko, T., “An Overview of Semidiscretization and Time integration Procedures,” in *Computational Methods for Transient Analysis*, edited by T. Belytschko and T. J. R. Hughes, North-Holland, 1983, pp. 1–65.
9. Anderson, A., Cooper, B., Neely, R., Nichols, A., Sharp, R., and Wallin, B., *Users Manual for ALE3D*, Lawrence Livermore National Laboratory, Ver. 3.4, 2003.
10. Steinberg, J., “Equation of State and Strength Properties of Selected Materials,” UCRL-MA-106439, 1996.
11. Catalano, E., McGuire, R., Lee, E. L., Wrenn, E., Ornellas, D., and Walton, J., “The Thermal Decomposition and Reaction of Confi ned Explosives,” in *Proceedings of 6th International Detonation Symposium*, Coronado, CA, Offi ce of Naval Research, pp. 214–222, 1976.
12. Prior, A. M., “Applications of Implicit and Explicit Finite Element Techniques to Metal Forming”, *J. of Material Processing Technology*, **45**, pp. 649–656, 1994.